Multi-Objective Optimization of Cellular Scanning Strategy in Selective Laser Melting

Ali Ahrari, Kalyanmoy Deb
Michigan State University
East Lansing, MI, USA
aliahrari1983@gmail.com
kdeb@egr.msu.edu

Sankhya Mohanty, Jesper H Hattel
Department of Mechanical Engineering
Technical University of Denmark Kgs. Lyngby, Denmark
samoh@mek.dtu.dk
jhat@mek.dtu.dk

COIN Report Number 2017006

***Abstract*—The scanning strategy for selective laser melting – an additive manufacturing process – determines the temperature fields during the manufacturing process, which in turn affects residual stresses and distortions, two of the main sources of process-induced defects. The goal of this study is to develop a multi-objective approach to optimize the cellular scanning strategy such that the two aforementioned defects are minimized. The decision variable in the chosen problem is a combination of the sequence in which cells are processed and one of six scanning strategies applied to each cell. Thus, the problem is a combination of combinatorial and choice optimization, which makes the problem difficult to solve. On a process simulation domain consisting of 32 cells, our multi-objective evolutionary method is able to find a set of trade-off solutions for the defined conflicting objectives, which cannot be obtained by performing merely a local search. Possible similarities in Pareto-optimal solutions are explored.**

Keywords— scan strategies; additive manufacturing; residual stress; distortions

I. INTRODUCTION

Selective laser melting (SLM) is a class of additive manufacturing in which a highly-focused laser beam scan and melt a layer of gas-atomized metal power at selected places following a particular strategy. Because of the accuracy of the process and layer-by-layer fabrication, SLM allows for manufacturing of complex structures with internal features and thin walls, where traditional processes cannot be used. Like most additive manufacturing process, the setup cost is comparatively low, and thus it provides an alternative for easy prototyping and potentially direct manufacturing.

The current state-of-the-art machines implementing SLM process determine the aforementioned strategy based upon the geometry of the component being produced. As the manufacturing process involves building a component layer-by-layer, the machine typically receives a slice of the component as input, corresponding to the thickness of the layer being produced. Thereupon, the best-practice involves dividing the domain into randomly oriented islands (or cells) of similar or different sizes that are then processed using a randomly generated sequence but always following a parallel scanning strategy [1].

The chosen scanning strategy, however, directly affects the temperature field over the process, and therefore some research can be found in literature towards determining good scanning strategies [2] [3] [4] [5] [6] [7] [8] [9] [10]. The relative scarcity of research in this field is an outcome of the large computation time/resource requirements for solving the multi-scale multi-physics problem in selective laser melting. However, a few works [11] [12] exist that approach the optimization of scanning strategy as a heuristic problem, thereby achieving practical solutions within acceptable timeframes.

Prior activities towards optimizing cellular scanning strategy have adopted a single-objective formulation and implemented it across models of progressing complexity - leveraging the capability of each model to limit the parametric window within certain accuracy. Drawing upon earlier success, the current study seeks to develop a multi-objective approach towards optimizing the cellular scanning strategy to widen the scope of process optimization. As the focus of the current work is on identifying meaningful objective functions as well as assessing the performance of the optimizing algorithm, a simplified thermal model is used instead of a complex multi-physics model. As such thermal modeling forms the basis for analyzing the development of thermal stresses, predicting the growth of microstructures and mechanical properties in products manufactured using selective laser melting – and thus is a good starting point for implementing the evolutionary algorithms.

Recent advances in multi-objective optimization allows us to study the interaction of two or more conflicting objectives in practical problems like the SLM process. Here, we use a method following the principals of non-dominating sorting genetic algorithm (NSGA II) [13] to find multiple trade-off solutions in a single simulation. Results obtained from the optimization run are analyzed to find important information about how to create a good solution in a SLM process.

In the remainder of the paper, we present the numerical model description of the SLM process in Section II. Formulation of three objectives is provided in Section III. Details about the optimization algorithm are discussed in Section IV. Results from optimization runs are provided in Section V and conclusions of this study are made in Section VI.

II. Numerical Model Description

A simple 2D rectangular domain of size $l \times w$ and of thickness δ is considered for the current study. The domain is discretized such that the distance between two adjacent nodes in the x-y directions is δ, thereby resulting in cubic elements (Fig. 1). Starting with ambient temperature of $T=T_\infty$, a simple method based on finite difference is used to update the temperature field using the energy equation while assuming constant thermal properties:

$$k_0 \nabla^2 T + \dot{q}_V = \rho c_P \frac{\partial T}{\partial t}, \qquad (1)$$

where $T = T(x, y, t)$ is the transient temperature field, $\dot{q}_V$ is the equivalent heat applied with a laser beam of power P_{laser} to a domain exposed to convective cooling under ambient conditions, k_0 is the heat conductivity of the powder, ρ is the density of the powder, and c_P is the specific heat capacity of the powder. The time step size when solving the above equation system is chosen small enough to ensure that the laser beam affects each cubic element for several time steps, thereby increasing the accuracy of the temperature predictions especially when latent heat is to be considered, i.e. when melting/solidification occurs. The current thermal model neglects the temperature-dependence of material properties as well as the influence of material distribution in form of a powder bed; however, as stated earlier, the focus of the current study is development of the multi-objective optimization approach for which the current thermal model is adequate.

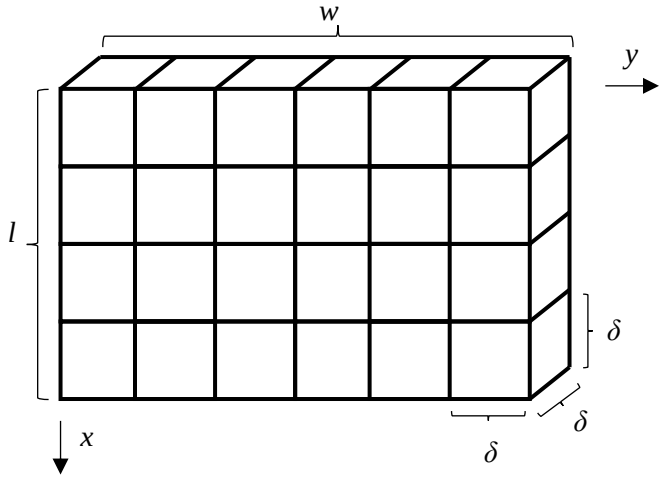

Fig. 1. A sample part consisting of 6×4 elements

III. Formulation of the Objectives

As a starting point, minimization of distortions and residual stresses are chosen as objectives for the optimization study. These two objectives are mechanical entities, and thus a method of quantifying them in terms of thermal entities is the first task. The following section deals with formulation of functions that can potentially give a measure of these defects.

A. Formulation for Residual Stresses

Prince Rupert's Drops [14] are an excellent example of how thermal residual stresses develop in materials subjected to high heating and cooling rates. In the absence of external anchoring/restraints, only regions with sufficiently high temperatures i.e. molten/soft regions that are self-constrained by solid regions can develop residual stresses upon solidification and cooling. As the dependence of the aforementioned phenomena on the gradient of temperatures is apparent, a reasonable objective can be:

$$f_1(\boldsymbol{\theta}) = \int_0^t \iint \left(\left|\frac{\partial T}{\partial x}\right| + \left|\frac{\partial T}{\partial y}\right| \right) \, dA dt. \qquad (2)$$

Using discretization technique, the above function can be approximated as follows:

$$f_1(\boldsymbol{\theta}) \propto \sum_{k=1}^{K} \sum_{j=2}^{J} \sum_{i=2}^{I} \begin{pmatrix} \left|T(x_i, y_j, t_k) - T(x_{i-1}, j, t_k)\right| \\ +\left|T(x_i, y_j, t_k) - T(x_i, y_{j-1}, t_k)\right| \end{pmatrix} \qquad (3)$$

This formulation implicitly penalizes isolated overheated regions because they result in a higher value for the average gradient of temperature. It is also expected to favor processing central regions before exterior regions as such scenarios would reduce the temperature gradients as compared to when exterior cells are processed first.

B. Formulation for Distortions

In the current study, the displacement of the powder due to thermal expansion, denudation and/or vapor expulsion are not considered. Thus, thermal expansion/contraction will result in displacement of the molten regions upon cooling and returning to the room temperature, which can cause distortions. Thermal displacement is proportional to increase in temperature and the size of the region subject to such an increase. Therefore, the average displacement is proportional to the average temperature difference between the part and ambient:

$$\Delta_{ijk} = \alpha\left(T(x_i, y_j, t_k) - T_\infty\right) \qquad (1)$$

in which α is the coefficient of thermal expansion of the powder. The cumulative displacement at any time $t=t_k$ can then be calculated as follows:

$$\overline{\Delta}_k = \sum_{j=1}^{J} \sum_{i=1}^{I} \Delta_{ijk} \qquad (2)$$

This cumulative displacement might affect the location of melting for the remaining parts (not melted so far) relative to the original process plan. Taking this into consideration, a measure of in-plane distortions during the SLM process can be obtained via the following formulation:

$$f_2(\boldsymbol{\theta}) = \sum_{k=1}^{T} \overline{\Delta}_k \times (t_{\mathrm{T}} - t_k) \tag{3}$$

C. Overheated Regions

Overheated regions negatively affect the quality of the final product [1] [10] [11]. Therefore, another potential objective can be minimization of the average number of elements that have become overheated during scanning:

$$f_3(\boldsymbol{\theta}) = \frac{1}{K} \sum_{k=1}^{K} \sum_{j=1}^{J} \sum_{i=1}^{I} c_{ijk} T(x_i, y_j, t_k), \tag{3}$$

$$c_{ijk} = \begin{cases} 0 & \text{if } T(x_i, y_j, t_k) < T_{\text{overheat}} \\ 1 & \text{otherwise} \end{cases}$$

in which T_{overheat} is a fixed value (approximated as mean of melting and boiling temperature) specifying the overheat temperature.

IV. Optimization Algorithm

In the current study, a real-valued genetic algorithm is used to optimize the scanning path with respect to the objective functions. Unlike previous studies [1] [9] [12], where the optimization problem was decomposed into two sub-problems, in the current study optimization of the scanning sequence and the scanning strategy for each cell is performed at the same time. While the previous studies chose to split the optimization problem into sequential optimization of sub-problems so as to reduce the computation requirements, the quality of the optimized solutions can undoubtedly be improved by treating both the sequence and cell strategy together. The operators of the developed method are defined as follows.

A. Representation

Following the methodology employed in [1], the 2D region is divided into $N_{\mathrm{l}} \times N_{\mathrm{w}}$ cells (see Fig. 2). Each cell consists of several elements which are scanned one after another until the whole cell is scanned by the laser. In the current study, each cell may be scanned using one of the following six scanning strategies (Fig. 3):

1) Paralleled vertical
2) Parallel horizontal
3) Anti-paralleled vertical
4) Anti-parallel horizontal
5) Out-Spiral
6) In-Spiral

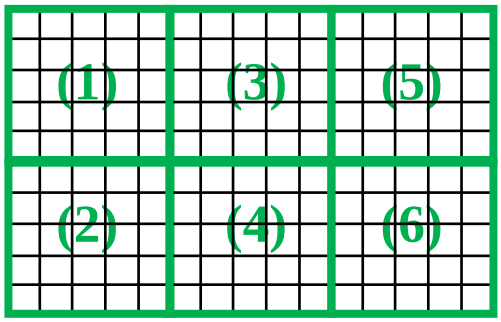

Fig. 2. The part is divided into cells each cell, which consists of several elements (25 in this illustration), may be scanned different than the other cells. For this illustration, N_{l}=2, N_{w}=3 and there are 25 elements in each cell.

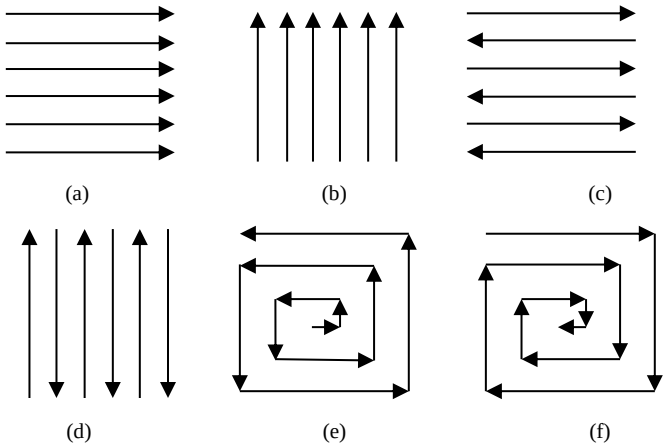

Fig. 3. Illustration of different scanning strategies: a) Parallel horizontal b) parallel vertical c) Anti-parallel horizontal d) Anti-parallel vertical e) Out-Spiral and f) In-Spiral

To configure the overall scanning path, the scanning sequence of the cells and the scanning strategy for each cell needs to be defined. Therefore, each candidate solution is represented by two vectors: $\boldsymbol{\theta}=\{\boldsymbol{q}, \boldsymbol{s}\}$:

- Elements of $\boldsymbol{q}$ are Natural numbers determining sequence of the scanning of the cells.
- Elements of $\boldsymbol{s}$ specify the scanning strategy for each cell.

$\boldsymbol{q}$ and $\boldsymbol{s}$ have $N_{\mathrm{l}} \times N_{\mathrm{w}}$ elements each. For a feasible design, $\boldsymbol{q}$ must be a permutation of Natural numbers from 1 to $N_{\mathrm{l}} \times N_{\mathrm{w}}$.

B. Recombination

Since each candidate solution is composed of two types of design variables, two types of recombination operators are necessary. For the unit cell scanning strategy, $\boldsymbol{s}$, the standard two-point crossover is used, given that the obtained offspring are always acceptable since each variable may take any integer between 1 and 6 inclusive; however, for the sequence of scanning $\boldsymbol{q}$, a recombination specialized for combinatorial optimization is required. The following recombination operators for $\boldsymbol{q}$ have been considered:

- Partially Mapped Crossover (PMX)

- Order- Based Crossover (OX1)
- Cycle Crossover
- Priority crossover
- Specialized crossover

Cycle, PMX and OX1 are well-known crossover operators for combinatorial problems [15]. The other two crossover operators are explained in this section. For all the crossovers, two parents are selected using tournament selection. The crossover operator is then applied with a probability of P_c.

1) Priority crossover: The idea unfrtlying priority crossover is that the sequence of the cells indicates their priority, which is inherited by the offspring. For example, for the case with six cells illustrated in Fig. 4, cell #3 is the first cell to be scanned. This means it has the highest priority for scanning, which is 6. An offspring inherits the priorities from their parents. The priority of each cell of offspring is the weighted average of priorities of the corresponding cells in the parents. The offspring ($\boldsymbol{q}_3$) can be generated when its priorities are known.

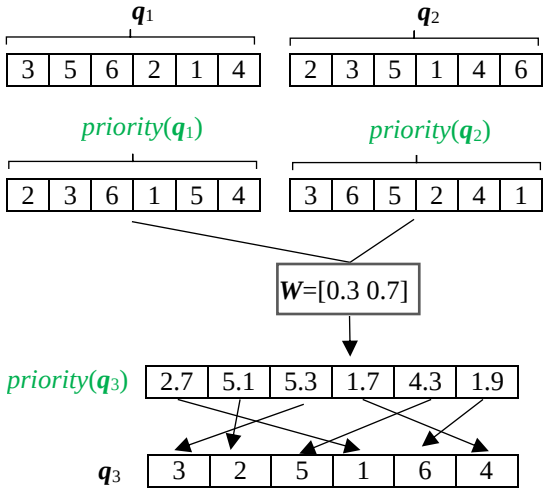

Fig. 4. The priority crossover. From top to bottom: two parent's $\boldsymbol{q}_1$ and $\boldsymbol{q}_2$ are selected for recombination. The priority of each cell is calculated for each parent. A random weight vector calculates the contribution of the priorities of each parent in generating the priorities of the new child. The child ($\boldsymbol{q}_3$) is generated by sorting the cell numbers according to their priorities.

One advantage of this type of crossover is that it can easily be generalized to an arbitrary number of parents. For this study, the number of parents was fixed to be two, to provide a more similar setting to other crossover operators. For each pair of parents, two random weight vectors were selected to generate two offspring.

2) Specialized crossover: The specialized crossover uses information on 2D arrangement of the cells in this problem. The goal of this crossover is to preserve adjacency of cells considering 2D heat conduction in the part. Proper use of problem-specific knowledge can result in significant improvement in efficiency of EAs especially for large-scale problem (see [16] and [17] for examples). This crossover is summarized in Fig. 5 for N_l=5 and N_w=4. First, a square of arbitrary size is selected, e.g. the region highlighted in gray. The selected region in both parents might contain common numbers, such as those shown in bold. The numbers in the cells inside the selected square region are transferred to the offspring directly (Fig. 5(b)). Finally, the remaining numbers are assigned to the remaining cells, from top to bottom and left to right (Fig. 5(c)). This type of crossover resembles OX1; however, the selected cells for direct transfer to the offspring are inside a square.

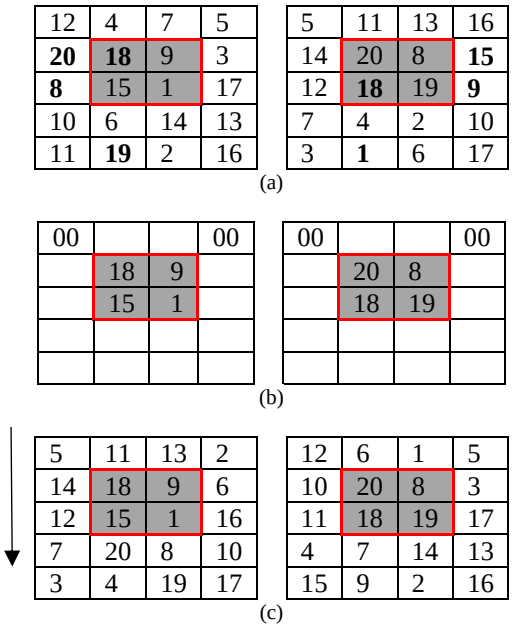

Fig. 5. Specialized crossover introduced for 2D cellular scanning.

C. Mutation

Each element is mutated with a probability of P_m. We use random swap for elements of $\boldsymbol{q}$, which randomly selects another element and switches the values of the two elements. For elements of $\boldsymbol{s}$, the mutation operator replaces the unit cell scanning strategy with another strategy. For mutation of the unit cell scanning strategies, a higher probability is assigned for mutation to a more similar strategy. Based on Fig. 3:

- Strategies (a) and (c) are more similar to each other than to other strategies.
- Strategies (b) and (d) are more similar to each other than to other strategies
- Strategies (e) and (f) are more similar to each other than to other strategies

The value of each mutated cell may change to any integer between 1 and 6 (inclusive) but the current value, with dissimilar probabilities:

- The probability of mutating the scanning strategy to a more similar strategy is 1/3.

- The probability of mutating the scanning strategy to any other strategy is 1/6.

D. *Selection*

The non-dominated sorting of NSGA-II [13] is applied for selection procedure. Thus, solutions with a lower non-domination rank are selected, and for two non-dominating solutions, the one with a greater crowding distance is preferred. For details of NSGA-II, readers are referred to [13].

V. Results and Discussion

Preliminary results revealed that the values of the second defined objective function are almost similar for every solution. A possible reason can be the high speed of the process that leaves little time for heat transfer to the ambient air i.e. the process is conduction-dominated in the simulated time window. Therefore, the average temperature of the part at identical times is similar for all designs. Consequently, only the first and the third objectives are considered for subsequent studies.

For thermal analysis, the following parameter setting are used:

- l=8 mm, w=4 mm, N_l=8, N_w=4, δ=0.1 mm, T_∞=150 ˚C
- P_{laser}=120W, dt=12.5 µs, V_{laser}=800 mm/s
- h=7 W/m^2.K, k=50 W/m.K, ρ=7850 Kg/m3,
- Latent melting heat was assumed to be 1260 J/Kg

In the first stage, a parameter study with limited evaluation budget and only five independent runs is performed to compare the effect of the aforementioned crossover operators and select the most successful ones. In the second stage, a greater evaluation budget is used with the most successful crossover operator for the problem to find the (near-) Pareto-optimal solutions. A local search to check optimality of the obtained solutions is also performed.

A. *Finding the Best Crossover Operator*

The following parameter setting are used:

- *TourSize*=2 (Tournament size for selection)
- *MaxIter* = 600 (Maximum number of iterations)
- *PopSize*=100 (Population size)
- P_c=0.85 (Crossover probability)
- P_m=1/32 (Mutation probability)

The five different crossover operators (PMX, OX1, Cycle, Priority and Specialized) discussed earlier are applied. For each crossover operator, five independent runs are performed. A method based on Normal Constraint [18] is used to select 100 uniformly distributed solutions on the Pareto front. These representative solutions are the closest ones to 100 parallel lines which make an angle of 45° to the f_1 and f_3 axes (Fig. 6). This results in a more uniformly distributed representative solutions than the default crowding distance metric in NSGA-II. For each crossover operator, 100 representative solutions are selected over the union of the five independent runs. The representative solution for each crossover operator are plotted in Fig. 7. According to figure 7, OX1 is the most successful crossover operator, more specifically for solutions with $f_1 \leq 34$ it can be seen to outperform all other crossover operators.

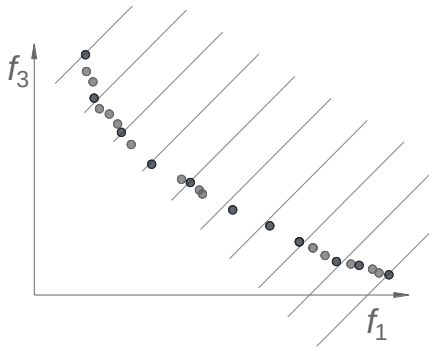

Fig. 6. Selection of the representative solutions (black circles) from all non-dominated solutions (all circles). For each line, the closest circles is selected as a representative solution.

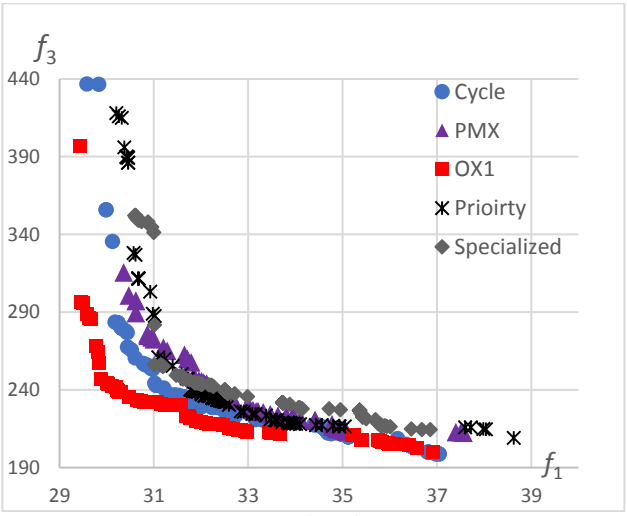

Fig. 7. Representative non-dominating front for each crossover operator

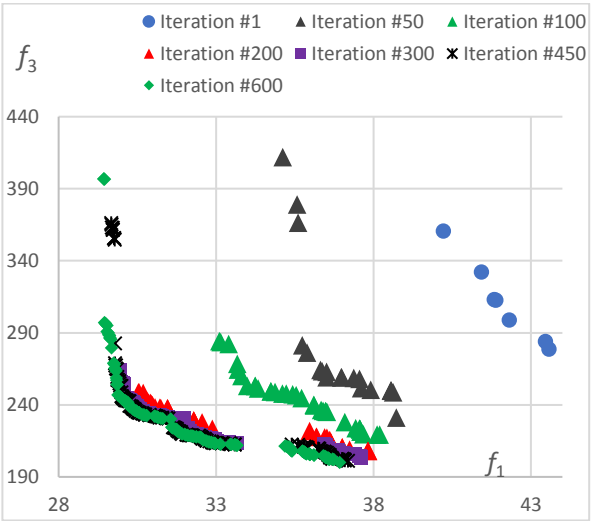

Fig. 8. Non-dominating solutions in selected interval of the optimization process when OX1 is selected as the crossover operator.

Fig. 8 illustrates the non-dominated front during the optimization when OX1 is employed as the crossover operator. As it can be observed, there is a huge improvement in non-dominating front up to the 200th iteration. Subsequent improvements are marginal, although still detectable. Therefore, terminating the optimization process at the 600th iteration, and possibly earlier, is a reasonable choice.

B. *High-Budgeted Simulations*

Based on the results in the prior section, it can be argued that using a larger population size can result in better non-dominating solutions by providing a stronger exploration of the search space, and can be particularly helpful if there are local Pareto-optimal solutions in the problem. Thus, the optimization process is repeated using a greater evaluation budget. Again, OX1 is employed as the crossover operator, since it emerged as the best crossover operator for the current problem. In comparison with the previous experiments, the population size is increased by four times (i.e. to 400) and a slightly greater value for the number of iterations (*MaxIter* =1000) is used. Other control parameters are as before. Twenty independent runs are performed, and the representative non-dominating front over the union of these runs is selected. Furthermore, local search is performed around these selected solutions to reach (local) Pareto-optimal solutions, as follows:

For each representative solution, the scanning sequence of each pair of cells is swapped and the new design is evaluated each time (32×31/2 = 496 evaluations). Similarly, all unit cell scanning strategies are implemented for each cell, one after another (32×5=160 evaluations). During this process, the representative solution is updated whenever a dominating solution is found. If 160+496=656 successive evaluations do not result in a new dominating solution, the local search is terminated, since it cannot find a better solution. The final solution can be considered as a Pareto-optimal solution, since variation in no single design parameter may result is a dominant solution. In addition to representative solutions from NSGA-II, the local search is performed for 400 randomly generated solutions as well. These solutions are plotted in the objective space in **Error! Reference source not found.**.

Some possible features shared among Pareto-optimal solutions are explored by analyzing the distance between pairs of successively scanned cells. The normalized move length is calculated by dividing this distance by the cell's edge length (0.1 mm). The histograms of the normalized move lengths for all pairs of successively scanned cells in 100 Pareto-optimal solutions are plotted in Fig. 10.

Finally, suitability of each scanning strategy for each cell is investigated by analyzing the Pareto-optimal solutions. The frequency of a scanning strategy for each cell in all 100 Pareto-optimal solutions is calculated. Since there are six possible options and 100 designs, the probability that the scanning strategy *m* appears in *n* solutions by chance follows a Binomial distribution. The expected value for each scanning strategy is 100/6. It is extremely unlikely that for the cell scanning strategy *m*, we have $n \geq 41$ ($P\ (n \geq 41) \leq 10^{-8}$); therefore, if it happens, it can be concluded that it is very likely that that particular cell is scanned with strategy *m*. Conversely, if for a particular cell a scanning strategy appears in none of the Pareto-optimal solutions ($P\ (n = 0) \approx 1.2\times10^{-8}$), we conclude that strategy *m* is unlikely to be suitable for that cell. Suitable and unsuitable choices for each cell are determined and illustrated in Fig. 11.

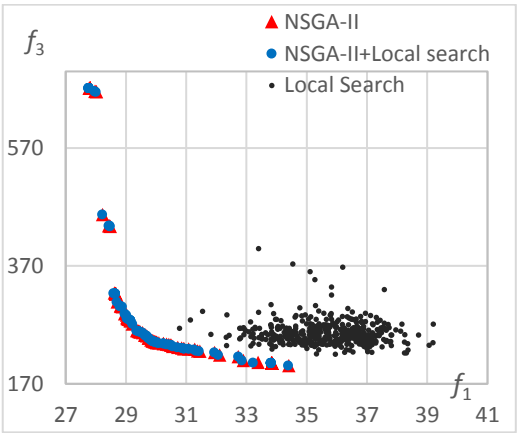

Fig. 9. Representative non-dominating solutions obtained using 20 independent runs of NSGA-II with a high evaluation budget, and those obtained after performing local search on these solutions. The small gray circles are locally optimized solutions which were randomly initialized.

- Fig. 9 illustrates that performing local search on the NSGA-II final solutions results in insignificant improvement. This implies that NSGA-II was successful at finding at least local Pareto-optimal solitons. There is a considerable gap between the fitness of 400 locally optimized random solutions and those obtained by NSGA-II. This implies performing a local search is unlikely to result in Pareto-Optimal solutions. Reaching diverse solutions on the Pareto front by local search is much less likely.
- The representative front displays a trade-off between the objectives which can help decision making on the canning path. A knee is quite often known as the best trade-off between the objectives, which can be noticed at $f_1 \approx 29.5$ in the current case.
- Fig. 10 demonstrates that the scanning path in Pareto-optimal solutions follow some specific rules. For example, moving from one cell to an adjacent cell which only shares a corner is very likely in Pareto-optimal solutions, as opposed to cells which share an edge. The frequency of such movement is more than 4 times in Pareto-optimal solutions than in randomly generated solutions (Such a movement results in a normalized move length of 1.41). From a thermal physics perspective, moving from one cell to the adjacent cell, which share an edge, concentrates the heat, resulting in increased temperature and superheated regions. Conversely, long distance jumps from one cell to another cell, with normalized move length of 3.5 or greater is also very unlikely to happen in a Pareto-Optimal solutions. Moving from a cell to a very distant cell results in two temperature peak in the temperature field, and thus increasing the average temperature

gradient. It seems that the best scanning path should start from one side and gradually move to the other side, but it should not scan edge-sharing cells successively. An important factor to consider about longer jumps, however, is that the results are based on the current definition of the objective functions, which inherently penalizes the occurrence of two temperature peaks at a distance; however, in real practice, such temperature peaks do not necessarily imply inferior or superior scanning strategies. Thus, the importance of formulation of objective functions is highlighted by these results. For the current problem, the chosen objective function of average gradients would lead to more conservative choices of scanning strategy than the case wherein direct gradient values are considered. The advantage of the current objective function lies in the lower optimization problem complexity and thereby considerably lower computational run-times.

- Fig. 11 illustrates that certain strategies should not be selected for specific cells. For example, spiral inward (scanning strategy #6) should not be selected for the eight cells in the left. Conversely, some strategies are likely to be selected for specific cells.
- The similarities among the Pareto-optimal solutions can be used for identifications of rules that govern the Pareto-optimal solutions and can be utilized to improve efficiency of the optimization by repairing bad solutions, which is known as "innovization" [19].

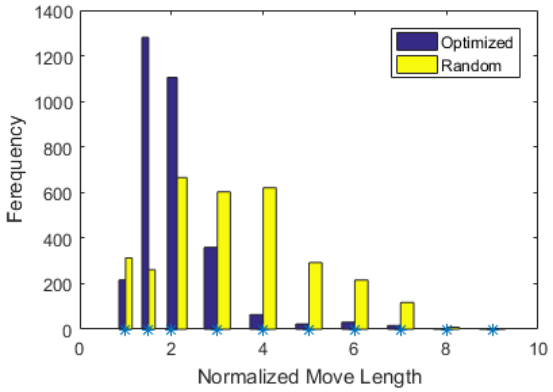

Fig. 10. Distribution of the normalized move length for 100 Pareto-Optimal solutions from NSGA-II plus local search and 100 random solutions.

- 6	5,3 6,4,2	0 6	5,4 3,2,1	6 -	3 5,4,2	3 2	- 3,2
2 6,4	1 6,4,3	5 6	5 2,1	- -	3 6,5,4,2	3 6	5 2
3 6,2	1 6,4,2	5 6,2	5 4,3	3 5	3 6,5,4	4 2	5 1
5 6,4,2	5 6,4	- 6	5 -	3 5,4,2	3 6,4,2	- 2,1	5 3,1

Fig. 11. Statistical analysis of the scanning strategies in 100 Pareto-optimal solutions obtained from NSGA-II + local search. For each cell, the upper number (green) represents the strategy that is likely to be present in a Pareto-optimal solution, while the numbers in the 2nd row refers to the strategies that are unlikely to be present in a Pareto-optimal solution.

VI. Summary and Conclusions

This study has developed a method for multi-objective optimization of the scanning path in selective laser melting (SLM), one of the main methods for additive manufacturing of metals. The goal has been to minimize the induced defects in the product by proper selection of the scanning path. The 2D plate has been divided into multiple cells which may be scanned using one of the available strategies. Three objective functions were introduced to predict the mechanical defects in the product based on analysis of the transient temperature field, but one of them has been found to be not sensitive to the trade-off in other two objectives. The scanning sequence of the cells and the employed strategy for each cell have been kept as variables to the optimization problem

Despite the usage of a simplified thermal model, interesting results regarding trade-off between different objectives have been observed. Presence of local Pareto fronts in this problem has posed a challenge and has encouraged us to try different crossover operators. Using a purely local search method failed to reach a near-global Pareto-optimal solution, which highlights advantages of EAs for this problem.

A dateable similarity between the Pareto-optimal solutions has been observed – a task which has been called as "innovization" in other multi-objective application studies. For example, the distance between two successively scanned cells is usually in a narrow limit when Pareto-optimal solutions are considered. Edge-sharing cells or distant cells should not be scanned one after another. Specific scanning strategies turned out to be good choices for specific cells while some other strategies should not be used for those cells.

It is interesting that we have observed a knee region in the obtained trade-off front, thereby making the knee region a preferred region for decision-making. While justifications for formulation of different objective functions have been provided, further experimental analysis of suitability of these functions can provide practical solutions, especially if they are able to predict defects in the final products. Also, as an immediate extension, the developed formulations of objectives will be used along with more rigorous numerical SLM process models to verify and validate the results from the multi-objective optimization procedure. These can be the subjects of future research in the domain of this study.

VII. Acknowledgments

Computational work in support of this research was performed at Michigan State University's High Performance Computing Facility. Authors acknowledge the financial support provided by REWIND consortium project from Danish Council of Strategic Research through Technical University of Denmark.

This work is accepted for presentation in IEEE CEC'2017. Please refer to the conference proceeding for citation.

REFERENCES

[1] S. H. J. Mohanty, "Cellular scanning strategy for selective laser melting: Capturing thermal tends with a low-fidelity, pseudo-analytical model',," *Mathematical Problems in Engineering*, no. 715058, 2014.

[2] C. Hauser and T. Childs, "Raster scan selective laser melting of the surface layer of a tool steel powder bed," *Proceedings of the National Academy of Sciences of the United States of America*, vol. 103, no. 4, pp. 379-384, 2006.

[3] R. Stamp and P. Fox, "The development of a scanning strategy for the manufacture of porous biomaterials by selective laser melting," *Journal of Material Science*, pp. 1839-1849, 2009.

[4] W. Zhang, Y. Shi, B. Liu, L. Xu and W. Jiang, "Consecutive sub-sector scan mode with adjustable scan lengths for selective laser melting," *International Journal of Advanced Manufacturing Technology*, vol. 41, no. 7-8, pp. 706-713, 2009.

[5] T. Antignac, J. Jhabvala, E. Boillat and R. Glardon, "On the effect of scanning strategies in the selective laser melting process," *Virtual and Physical Prototyping*, vol. 5, no. 2, pp. 99-109, 2010.

[6] B. E. A. T. G. R. Jhabvala J., "Study and simulation of different scanning strategies in SLM," in *Innovative Developments In Design And Manufacturing*, Taylor & Francis Group, 2010, pp. 369-375.

[7] B. Qian, F. Han, Y. Shi and Q. Wei, "Comparison of two scan strategies applied to the selective laser melting," in *International Conference on Computer Application and System Modelling*, 2010.

[8] Y. Shi, Q. Wei, B. Qian and H. Wang, "The helix scan strategy applied to the selective laser melting," *International Journal of Advanced Manufacturing Technology*, vol. 63, no. 5-8, pp. 631-640, 2012.

[9] S. Mohanty, C. Tutum and J. Hattel, "Cellular scanning strategy for selective laser melting: evolution of optimal grid-based scanning path and parametric approach to thermal homogeneity," in *Proceedings of SPIE 8608, Laser-based Micro- and Nano-packaging and Assembly VII*, San Francisco, USA, 2013.

[10] R. Mertens, S. Clijsters, K. Kempen and J. Kruth, "Optimization of Scan Strategies in Selective Laser Melting of Aluminum Parts With Downfacing Areas," *J. Manuf. Sci. Eng.*, vol. 136, no. 6, 2014.

[11] S. Mohanty and H. JH, "Cellular scanning strategy for selective laser melting: Generating reliable, optimized scanning paths and processing parameters," *Proceedings of SPIE (ISBN: 9781628414431), 2015, SPIE - International Society for Optical Engineering,*, vol. 9353, no. 93530U, p. 13, 2015.

[12] S. Mohanty and J. Hattel, "Reducing residual stresses and deformations in selective laser melting through multi-level multi-scale optimization of cellular scanning strategy," *Proceedings of SPIE: Laser 3D Manufacturing III*, vol. 9738, no. 97380Z, p. 12, 2016.

[13] K. Deb, A. Pratap, S. Agarwal and T. A. M. T. & Meyarivan, "A fast and elitist multiobjective genetic algorithm: NSGA-II," *IEEE transactions on evolutionary computation*, vol. 6, no. 2, pp. 182-197, 2002.

[14] L. Brodsley, C. Frank and J. W. Steeds, "Prince Rupert's drops," *Notes and Records of the Royal Society*, vol. 41, no. 1, pp. 1-26, 1986.

[15] A. J. Umbarkar and P. D. Sheth, "Crossover Operators in Genetic Algorithms: a review," *ICTACT Journal on Soft Computing*, vol. 6, no. 1, pp. 1083-1092, 2015.

[16] A. Ahrari and K. Deb, "An improved fully stressed design evolution strategy for layout optimization of truss structures," *Computers & Structures*, vol. 164, pp. 127-144, 2016.

[17] K. Deb and C. Myburgh, "Breaking the Billion-Variable Barrier in Real-World Optimization Using a Customized Evolutionary Algorithm.," in *GECCO*, Denver, 2016.

[18] A. Messac and C. A. Mattson, "Normal constraint method with guarantee of even representation of complete Pareto frontier," *AIAA journal*, vol. 42, no. 10, pp. 2101-2111, 2004.

[19] K. Deb, Innovization: discovering innovative solution principles through optimization, Springer , 2014.

[20] S. Mohanty and J. H. Hattel, "Optimization Of Cellular Scanning Strategy For Selective Laser Melting," DTU.

[21] L. Davis, Handbook of genetic algorithms., New York: Van Nostrand Reinhold, 1991.

[22] D. E. Goldberg, Genetic algorithms in search, optimization and machine learning, Addison-Wesley, 1989.